Chem Soc Rev

TUTORIAL REVIEW

View Article Online
View Journal | View Issue

Cite this: *Chem. Soc. Rev.*, 2014, **43**, 1800

Supramolecular reactivity in the gas phase: investigating the intrinsic properties of non-covalent complexes

Luca Cera and Christoph A. Schalley*

Received 14th October 2013

DOI: 10.1039/c3cs60360a

www.rsc.org/csr

The high vacuum inside a mass spectrometer offers unique conditions to broaden our view on the reactivity of supramolecules. Because dynamic exchange processes between complexes are efficiently suppressed, the intrinsic and intramolecular reactivity of the complexes of interest is observed. Besides this, the significantly higher strength of non-covalent interactions in the absence of competing solvent allows processes to occur that are unable to compete in solution. The present review highlights a series of examples illustrating different aspects of supramolecular gas-phase reactivity ranging from the dissociation and formation of covalent bonds in non-covalent complexes through the reactivity in the restricted inner phase of container molecules and step-by-step mechanistic studies of organocatalytic reaction cycles to cage contraction reactions, processes induced by electron capture, and finally dynamic molecular motion within non-covalent complexes as unravelled by hydrogen–deuterium exchange processes performed in the gas phase.

Key learning points
- Find out how a mass spectrometer can be used as a laboratory to investigate the reactivity of supramolecules beyond their analytical characterization
- Learn about using mass spectrometry for the examination of the intrinsic properties of supramolecules
- Understand why and how supramolecular reactivity is significantly different in solution and in the high vacuum of a mass spectrometer
- Get an idea of the intramolecular reactivity of supramolecular complexes rather than the prominent exchange processes usually observed in solution

1 Introduction

Supramolecular reactivity could simply be defined as the formation and dissociation of non-covalent bonds. This statement is as clear-cut as one would probably expect a definition to be. It is also general enough to cover all the different phenomena that are connected with supramolecular reactivity. However, this is why it constitutes a problem at the same time: it neglects the broad variety of phenomena that are connected to non-covalent bonding. The formation and dissociation of non-covalent bonds range from the elusive contacts between molecules and the surrounding solvents to strong and sometimes kinetically quite stable coordinative bonds. The phenomena that rely on non-covalent bonds cover molecular recognition, when selective binding events are encountered, self-assembly and self-sorting, when a potentially complicated mixture turns into one or only very few of the many possible species, template effects, which organize reaction partners in space and thus influence their reactivity, catalysis based on changes in molecular reactivity induced by non-covalent bond formation, and many other functions requiring the combination of the usually high dynamics of non-covalent bonds and their ability to organize molecules in space and in time.

Beyond analytics, modern mass spectrometry provides methods to investigate the supramolecules of interest under environment-free conditions. In the high vacuum inside the mass spectrometer, their intrinsic properties are accessible and can then be compared to the situation in the condensed phase. Many early studies that have been summarized previously[1] were devoted to structural aspects of supramolecular assemblies using, for example, fragmentation pathways of mass-selected ions in the gas phase as a structure-indicative tool. Among others, the topology of mechanically interlocked architectures[2] like rotaxanes, catenanes, or knotanes and the closed capsular structure[3] of hydrogen bonded or metallo-supramolecular containers with guest molecules inside were supported by tandem MS experiments. In these experiments, the desired ions are first generated, then isolated in a mass-selection step and finally fragmented by either collisions or laser irradiation. With appropriate

Institut für Chemie und Biochemie, Freie Universität Berlin, Takustraße 3, 14195 Berlin, Germany. E-mail: christoph@schalley-lab.de; Fax: +49 30 838 55367; Tel: +49 30 838 52639

isotope labelling strategies, even diastereomeric architectures such as the serine octamer[4] with its strong preference for homochiral cluster formation can be analysed. Besides structure, fundamental binding studies have been done and thermodynamic data[5] have been obtained for many non-covalent complexes.

When it comes to supramolecular reactivity, the investigation of non-covalent complexes in the gas phase promises a simplification in that the environment does not complicate the situation as it does in solution or the solid state. In addition, the isolation of the ions under study efficiently avoids any of the quick exchange processes of building blocks between the complexes. As they are all charged either positively or negatively, no direct reactions between them occur. This opens a completely new view into supramolecular reactivity as one starts to observe the intramolecular reactions within the complexes that are difficult to detect in condensed phase because they are superimposed by the many quick exchange processes.

Often, it is believed that gas-phase studies do not have much relevance to supramolecular chemistry in the condensed phase and thus are somewhat esoteric in nature. This is probably true, if one aims directly at economically useful applications. However, the additional knowledge obtained from these studies about fundamental binding processes, the nature of different types of non-covalent bonding or the more in-depth characterization of supramolecular complexes complementary to solution methods is valuable for innovation in this field.

To understand how the reactivity of supramolecular complexes changes when going from solution to the gas phase, the absence of competitive solvent molecules needs to be taken into account which leads to a significant increase of the strength of almost all non-covalent interactions – with the notable exception of the hydrophobic effect, of course. A particularly striking example is certainly the Coulomb interaction between a single Na^+ and a single Cl^- ion. The ion pairing energy in water is less than 10 kJ mol^{-1} because of the solvent's large dielectric constant and its ability to form hydrogen bonds with the chloride, while it is almost 700 kJ mol^{-1} in the gas phase. This is important, because the stronger non-covalent interactions in the gas phase make new reactivity possible, which would not occur in solution as the energy difference between formation and cleavage of non-covalent bonds as compared to covalent bonds is significantly diminished. More energy-demanding processes which cannot compete in solution with non-covalent bond formation and dissociation may do so in the gas phase.

In the present review, we focus on a few selected examples which highlight different aspects of supramolecular reactivity in the gas phase. Among them are the formation and cleavage of covalent bonds in non-covalent complexes, the reactivity in the restricted inner phase of container molecules, step-by-step mechanistic studies of organocatalytic reaction cycles, cage contraction reactions, processes induced by electron capture, and the highly dynamic molecular motion within non-covalent complexes as unravelled by hydrogen–deuterium exchange processes performed in the gas phase.

2 Tandem mass spectrometric experiments

The reactivity of gaseous ions in general and of ionized supramolecular complexes in particular is closely related to structural and energetic aspects. Quite often, special fragmentation patterns allow us to draw conclusions on the relative energy demand of competing reactions as well as structural details of the complexes under study. Although we will emphasize the reactivity aspect here, one should always consider all three aspects – structure, reactivity, and energetics – together to finally arrive at a concise interpretation of the data.

Luca Cera

Luca Cera received his MSc in Chemistry from the University of Milano Bicocca (Italy). After spending a year in London in the laboratory of Steven Goldup, where he got acquainted with supramolecular chemistry, he joined the Schalley group at the Freie Universität Berlin in 2012 to start his PhD education. He is currently focusing his research on the synthesis and FTICR mass spectrometric characterization of cucurbituril-based pseudorotaxanes aiming at the design and investigation of complex and stimuli-responsive molecular systems.

Christoph A. Schalley

Christoph Schalley studied chemistry at the University of Freiburg, Germany, and graduated in 1993 from the Technical University Berlin. In his PhD work with Helmut Schwarz at TU Berlin, he received his thorough education as a mass spectrometrist and gas-phase chemist. After postdoctoral work on supramolecular chemistry with Julius Rebek, Jr. at The Scripps Research Institute, La Jolla, USA, he combined both topics when he started his own research group as a habilitand at the University of Bonn. In 2005, he was appointed professor of organic chemistry at Free University Berlin. The Schalley group's research topics are diverse and comprise supramolecular chemistry in the gas phase as well as in solution and at interfaces.

Tandem MS experiments (MS^2) generally have four steps: ionization of the sample often producing a goulash soup of different ions, mass selection of the ion of interest as a purification step, the gas-phase reaction itself, *e.g.* a fragmentation or a bimolecular reaction, and finally the detection of the products. Depending on the instrument and ion abundance, product ions can also be reselected and subjected to a second, third, …, *n*-th gas-phase reaction (MS^n), for example to analyse consecutive fragmentation reactions. Bimolecular reactions are possible for example in ion trap or Fourier-transform ion-cyclotron-resonance (FTICR) mass spectrometers. FTICR mass spectrometers certainly combine a broad versatility of gas-phase experiments with high resolution and high mass accuracy. Nevertheless, the equipment and its maintenance is quite costly, so that less expensive instruments such as triple-quadrupole, ion trap or quadrupole-time-of-flight instruments are also frequently used.[6]

During the ionization process the integrity of the supramolecular structures should not be affected too much. Electrospray ionization (ESI) and – to a lesser extent – matrix-assisted laser desorption/ionization (MALDI) are two quite soft and frequently used ionization methods. In the MALDI procedure, the sample is dispersed and co-crystallized in an excess of a usually organic matrix and then subjected to a short laser pulse. The role of the matrix is to absorb the laser light and mediate the energy transfer from the laser to the sample. Furthermore, it often also ionizes the sample, for example by protonation. However, as the matrices are often competitive with the supramolecular interactions under study and because the ions may still have rather high internal energies after ionization, MALDI is somewhat limited for the ionization of supramolecules.

ESI is thus still the most often used ionization method. It allows transferring the analyte molecules into the gas phase directly from their native environment in solution – often even when quite unipolar solvents such as chloroform or dichloromethane are used. The sample is introduced into the ESI ion source dissolved in a volatile solvent through a metal-coated capillary that is maintained at high voltage (about 2 to 4 kV) to obtain charge separation. Charged droplets form at the tip of the so-called Taylor cone. Upon evaporation of solvent molecules from the droplets, which is often supported by desolvation and/or nebulizer gas flow, the droplets shrink. At the Rayleigh limit, at which the shrinking droplet cannot sustain the increasing density of charges anymore, either it can undergo Coulomb explosion into smaller droplets until finally desolvated ions form or individual ions may evaporate from the droplet surface. The choice of a suitable spray solvent can be crucial for successful ionization of supramolecules as solubility is one issue and the integrity of the supramolecular complex can be in danger, when solvent molecules compete with the non-covalent interactions.

Beyond these two most commonly used methods, other ionization techniques are available, which are specially devoted to weakly bound complexes. Among them, cryospray ionization (CSI)[7] was used to investigate self-assembly processes[8] and reaction intermediates using a cooled (variable-temperature) ion source.[9] Also, resonance-enhanced multiphoton ionization (REMPI) can be used to ionize very weakly bound supramolecular complexes which have been generated as very cold, gaseous neutrals by supersonic jet expansion.[10]

The mass-selection step – often called isolation – is performed differently in different mass spectrometers. In quadrupole instruments, only the ion of interest passes through on a stable trajectory defined by suitable settings of the direct and alternating voltages on the four rods of the quadrupole. Similarly, the voltages on the electrodes of ion traps can be tuned in a way that removes all unwanted ions from the trap. In a Fourier-transform ion-cyclotron-resonance (FTICR) mass spectrometer (Fig. 1), the ion cloud is kept on small orbits inside the analyser cell by a strong magnetic field. Every *m*/*z* value corresponds to one cyclotron frequency. Fourier transformation of the free induction decay (FID) which contains the superposition of all different cyclotron frequencies yields the mass spectrum. Undesired ions can be removed from the cell by selectively increasing their kinetic energy with suitable high-frequency electric fields to a level at which the orbit on which they circulate in the analyser cell is so large that they are neutralised at the cell walls. The FTICR cell can thus be used to trap the ions, to mass-select them, to allow them to react, and finally to detect them. Whatever the mass-selection principle is, it provides the means to pick a certain ion of interest from even complex mixtures and is thus comparable to a purification step in synthesis leading to a clean reactant which can then be used in the next reaction.

After mass-selection, the ions of interest can be subjected to a variety of different gas-phase experiments. Which experiments are available again depends on the type of instrument in which they are to be done; Fig. 1 shows a number of different experiments that can be conducted in an FTICR instrument[11] as an example. Collision-induced dissociation (CID) is one of the most widely used methodologies. The mass-selected ions are collided with a stationary collision gas, quite often noble gases

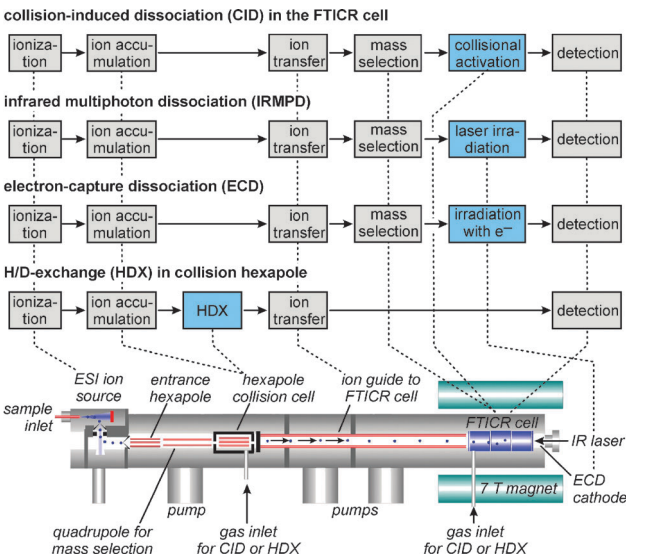

Fig. 1 The sequences of steps of different gas-phase experiments exemplarily shown for an FTICR mass spectrometer. Dotted lines indicate where in the mass spectrometer each step of these experiments is performed.

such as argon. In the collision, part of the ions' kinetic energy is converted into vibrational excitation followed by dissociation, when this excitation is strong enough. Alternatively, irradiation with laser beams – usually CO_2 lasers with 10.6 μm wavelength – in an infrared multiphoton dissociation (IRMPD) experiment can be used to afford the energy required for fragmentation. IRMPD is more efficient on larger ions as it depends on the presence of a band in the IR spectrum at the laser wavelength. If the ions are transparent at this wavelength (which is more likely for smaller ions), no excitation occurs. A third gas-phase experiment is the use of slow electron beams in electron-capture dissociation (ECD) experiments in FTICR instruments. Alternatively, electron transfer dissociation (ETD) from a suitable and independently generated anion radical can afford fragmentation in ion traps. Capture of an electron is only meaningful for multiply positive ions. In those, it leads to the formation of radical centres that usually react quite differently as compared to closed-shell ions. Fragmentation can also be induced by blackbody infrared radiative dissociation (BIRD).[12] In these experiments, the FTICR cell is heated and thus is a blackbody radiation source for the ions inside. By absorption and emission of IR photons, a thermal equilibrium between the cell walls and the ions is achieved so that their temperature is known. From these experiments, information on, for example, dissociation barriers of supramolecular complexes can be obtained. Also, bimolecular reactions are possible in ion traps and FTICR instruments. One prominent example is the exchange of labile hydrogen atoms against deuterium inside the mass spectrometer,[13] when mass-selected ions are subjected to reactions with exchange reagents such as ND_3, CH_3OD, or CH_3COOD.

An exciting technique which has become more and more widely available recently is ion mobility spectrometry (IMS).[14] In IMS instruments, the ions of interest are injected into a gas-filled drift tube and travel through the collision gas at low velocities. Fragmentation is thus not prominent. The larger the collision cross section of the ions, the later it arrives at the end of the drift tube. From the arrival time distribution, the collision cross sections can be determined. Comparison with, for example, theoretical cross sections obtained for various structures provides insight into the ion structures including supramolecular structures such as for example metallo-supramolecular assemblies[15] or the above-mentioned serine octamer.[16] As this method has mainly been used to obtain structural information, we do not include it in the present review.

This admittedly very brief discussion of experiments available to investigate gas-phase chemistry of supramolecular complexes clearly shows that modern mass spectrometers not only provide accurate analytical data, but also provide an arsenal of different methods to examine reactivity under the special circumstances of the gas phase.

3 Covalent bond cleavage competing with the dissociation of non-covalent bonds

As said above, supramolecular interactions are strengthened significantly in the absence of solvent. Consequently, covalent bond cleavages can sometimes efficiently compete with non-covalent bonds.[17] Fig. 2 shows an example in which this is even more likely the case, because the presence of two positive charges weakens the bonds because of charge repulsion. In such cases, charge-separating fragmentations are often observed as prominent signals in the mass spectra. It should be noted that such a process leads to two charged fragments both of which should be detected.

Two crown–ammonium pseudo[3]rotaxanes **Rot1** and **Rot3** are subjected to IRMPD experiments. The two pseudorotaxanes only differ by the bridge between the two binding stations along the axle and self-sort based on the crown ether ring size into a 1 : 1 : 1 complex of the diammonium axle, dibenzo[24]crown-8 **C8** and benzo[21]crown-7 **C7**.[18] When the ionization conditions are optimized for singly charged cations $[\mathbf{Rot1}\cdot 2H\cdot PF_6]^+$ and $[\mathbf{Rot3}\cdot 2H\cdot PF_6]^+$ the sequence of the crown ethers can be unambiguously determined by the subsequent dissociation of first **C7**, then HPF_6 and finally **C8**. No covalent bond cleavages are observed that compete with the dissociation of the supramolecular interactions.

However, when the dications $[\mathbf{Rot1}\cdot 2H]^{2+}$ and $[\mathbf{Rot3}\cdot 2H]^{2+}$ are mass-selected (Fig. 2), the cleavage of the anthracenyl methyl–N bond is observed. It should be noted that this bond is the only benzylic C–N bond in the axle, which leads to charge separation upon cleavage. Dissociation of one of the benzyl–N bonds next to the phenylene spacers would only bring the two charges closer together. Consequently, fragmentation of the axle is only observed next to the anthracene stopper.

The details are interesting: both doubly charged pseudorotaxanes first lose the smaller crown ether to give rise to the fragments at *m*/*z* 431 and *m*/*z* 499, respectively. No covalent bond cleavage is observed in competition with this reaction as the ammonium next to the anthracene is stabilized by solvation through **C8**. Before the benzyl–N bond is cleaved in the resulting $[\mathbf{Rot2}\cdot 2H]^{2+}$ fragment ion, **C8** first moves to the other binding site to form $[\mathbf{Rot2'}\cdot 2H]^{2+}$ as indicated by the formation of the fragment at *m*/*z* 671, in which the benzyl–N bond is cleaved, but **C8** is still present. This scenario changes significantly for $[\mathbf{Rot3}\cdot 2H]^{2+}$ with the longer spacer between the two binding stations. The longer spacer creates a higher barrier for the crown migration along the axle. Now, cleavage of the benzyl–N bond can efficiently compete with crown migration. The $[\mathbf{Rot4}\cdot 2H]^{2+}$ dissociates directly into three fragments: the anthracenyl methyl cation, the neutral crown and the axle fragment at *m*/*z* 359, which exclusively appears without crown ether complexed to it.

This example illustrates three aspects: (i) the competition of covalent and non-covalent bond cleavage depends not only on the strength of the supramolecular bond, but also on the charge state, which can significantly affect the strength of covalent bonds in a complex. Consequently, different charge states can be expected to yield very different fragmentation patterns. (ii) The charge repulsion in multiply charged ions and the stability of covalent bonds can also be significantly affected by supramolecular interactions and internal self-solvation as indicated by the fact that the benzylic C–N bond in $[\mathbf{Rot2}\cdot 2H]^{2+}$ dissociates only after crown movement, when the ammonium

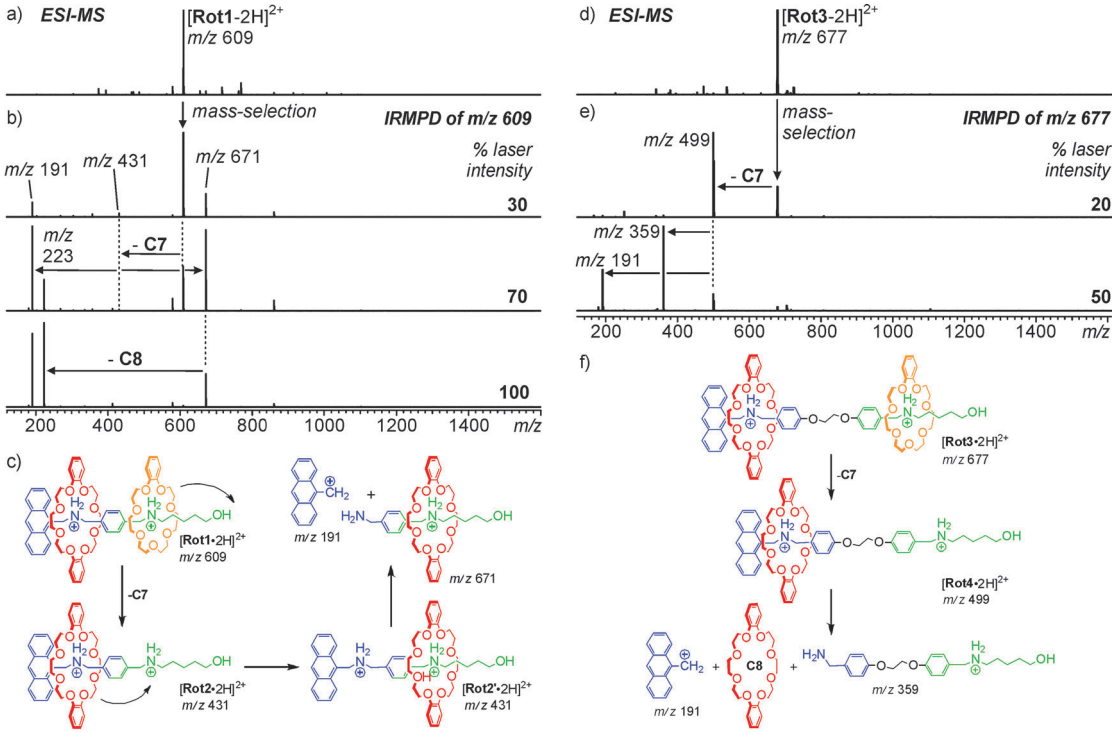

Fig. 2 The fragmentation reactions of two [3]pseudorotaxanes which differ only with respect to the length of the spacer between both binding stations on the axle. From top to bottom: ESI-FTICR mass spectra of **Rot1** (a) and **Rot3** (d), IRMPD experiments conducted with doubly charged parent ions [**Rot1**·2H]$^{2+}$ (b) and [**Rot3**·2H]$^{2+}$ (e), and mechanisms of the major fragmentation channels (c), (f).

ion is not stabilized by the crown anymore. (iii) A detailed analysis provides insight into fragmentation sequences and details of the reaction mechanisms and provides at least qualitative evidence for the relative energy demand of different reaction channels.

4 Mouse traps: covalent bond formation within non-covalent complexes

The opposite is also possible: Beauchamp *et al.*[19] were able to provide evidence for the formation of covalent bonds within a gaseous non-covalent complex (Fig. 3). The so-called ''mouse trap'', doubly crown-ether-substituted host molecule **5**, bears an azodiester group, which can quite easily form a carbene upon nitrogen loss. The two [18]crown-6 ethers provide binding sites that can be complexed by diammonium ions bridged with, for example, an alkyl chain long enough to bridge the two crown ether binding sites. Doubly protonated 1,6-diaminohexane (**DAH**) is a suitable example.

In the ESI mass spectrum of a mixture of **5** and **DAH**, doubly charged [**5**·**DAH**·2H]$^{2+}$ ions appear as the base peak (Fig. 3, top). Upon mass-selection and collisional activation in an MS/MS experiment (Fig. 3, centre), a nitrogen loss is more or less the only fragmentation product. This reaction thus proceeds below the dissociation limit of the complex – not surprisingly in view of crown–ammonium gas-phase binding energies in the range of 180 kJ mol^{-1}. Consequently, the expected carbene [**:5**·**DAH**·2H]$^{2+}$ indeed forms. The formation of covalent bonds between **5** and the **DAH** dication can be examined by an MS^3 experiment, in which the [**:5**·**DAH**·2H]$^{2+}$ ion is re-isolated and again subjected to collisional-activation (Fig. 3, bottom). As the proton affinities of primary ammonium ions and crown ethers are not too different ($\Delta PA \approx 20$–30 kJ mol^{-1}), a charge-separating fragmentation would easily be possible, if both components were still bound in a non-covalent way only. In this case, the [**DAH**·H]$^+$ and [**:5**·H]$^+$ fragments would be expected to occur more or less exclusively. However, the MS^3 spectrum clearly shows a large number of fragments that can be assigned to the cleavage of covalent bonds within the complex. This also provides evidence for the formation of a covalent bond between the two components – likely by insertion reactions of the carbene into one of the covalent bonds in the **DAH** guest dication.

This study provides clear evidence that the much stronger non-covalent interactions in the gas phase allow covalent bond formation to compete with complex dissociation. If such a reaction occurs, one can conclude the activation barriers for the covalent chemistry to remain below the dissociation threshold of the complex.

5 Inner-phase reactivity in the gas phase: reactions inside the cavities of cucurbiturils

Cucurbiturils[20] (Fig. 4, inset) are rigid, pumpkin-shaped macrocycles whose cavity size can be tuned systematically by the number of glycoluril monomers incorporated in their structure.

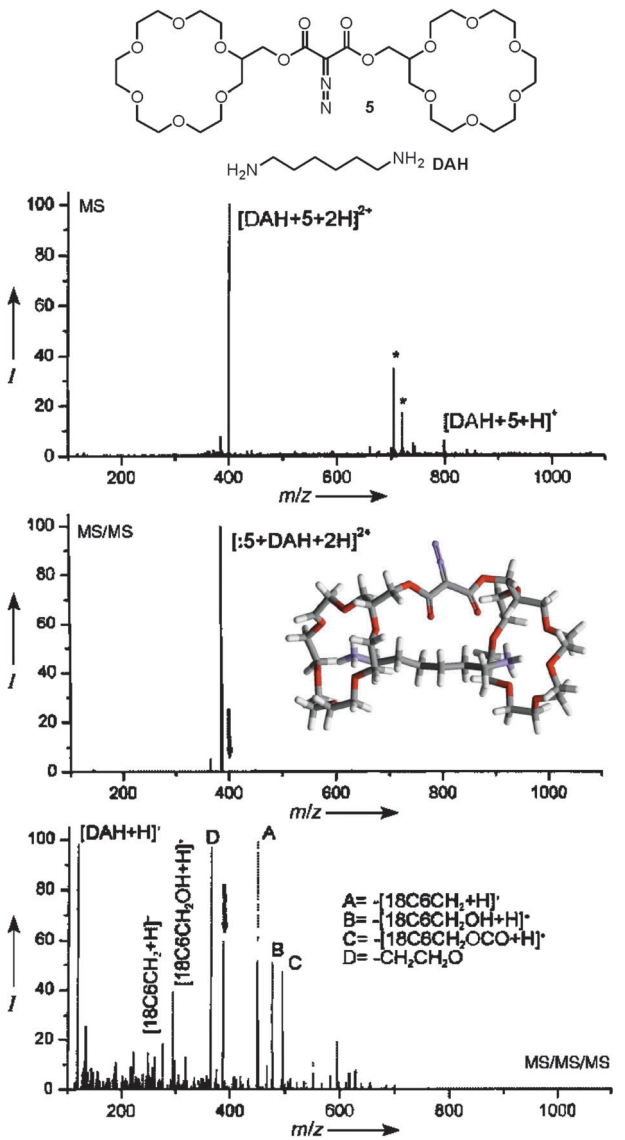

Fig. 3 Bis-crowned azodiester derivative **5** and guest diamine **DAH**. Top: ESI mass spectrum of a mixture of both compounds yielding the doubly charged [**DAH** + **5** + 2H]$^{2+}$ complex ion. Centre: MS/MS spectrum of mass-selected [**DAH** + **5** + 2H]$^{2+}$ showing almost exclusively the loss of N_2. Inset: optimized structure of the parent ion complex. Bottom: MS^3 experiment performed with the re-selected N_2 loss product ion. Reprinted from ref. 19 with permission from Wiley-VCH.

In solution, they have shown even catalytic activity.[21] Therefore, it is certainly interesting to investigate their inner-phase reactivity in the gas phase, where the cucurbituril complexes are isolated. In a recent, very elegant study,[22] Kalenius, Nau *et al.* have provided evidence that constrictive binding inside molecular containers can lead to a special reactivity in the gas phase.

Cucurbiturils **CB6–CB8** form protonated complexes with azoalkanes **6–8** (Fig. 4) – with the exception of the **CB6**/**7** and **CB6**/**8** pairs, in which the guest does not fit inside the cavity. The first step was to establish that indeed inclusion complexes rather than exclusion complexes are formed. Ion mobility mass spectrometry, which measures the collision cross sections of the ions under study, provided clear evidence for inclusion complexes: the protonated, empty cucurbituril exhibits the same collision cross section as the protonated host–guest complex. Based on this knowledge, the fragmentation reactions of all possible cucurbituril–azoalkane complexes were examined. Two fragmentation channels compete. One is the dissociation of the complex; the second corresponds to a retro-Diels–Alder reaction within the azoalkane and leads to the loss of neutral ethene and is followed for azoalkane **7** by further fragmentation reactions of the product as indicated in Fig. 4b.

Most interestingly, the balance between both channels – and with it the relative energy demand – is clearly dependent on the size complementarity of the cucurbituril cavity volume with that of the guest cation. For example, the [**CB7**·**6**·H]$^+$ ion predominantly reacts through the retro-Diels–Alder pathway, while smaller and more tightly packed [**CB6**·**6**·H]$^+$ as well as larger and more loosely packed [**CB8**·**6**·H]$^+$ fragment predominantly by complex dissociation.

From these trends, one can conclude that constrictive binding is on the one hand required as otherwise the dissociation of the host–guest complex occurs quite easily and covalent reactivity cannot compete efficiently. On the other hand, too tightly packed complexes do not react in retro-Diels–Alder reactions which are known to have a positive activation volume. In these cases, the transition state becomes less favourable in energy as it does not fit well into the cavity of the host.

6 Gas-phase organocatalysis

Supramolecular catalysis – nowadays usually considered the field in organocatalysis where non-covalent bonds are responsible for catalytic activity – is certainly an exciting field within supramolecular reactivity. While gas-phase studies of catalytic cycles involving transition metals as the catalytically active species have been reported for several decades,[23] the examination of supramolecular catalysis by mass spectrometric methods is not as far developed. This is even more surprising when one considers the advantages of the examination of catalytic cycles in the gas phase: each step of the cycle can be studied separately as one can choose which reactants to add to the reaction cell at what particular moment. Re-isolation of each intermediate provides a clean starting point for the next step in the cycle.

Fig. 5 illustrates a recent example.[24] The complexes of larger, protonated crown ethers were observed to mediate the losses of propene from propylamine. The experiment proceeds in several steps. First, a propylammonium–crown complex is generated by electrospray ionization of a slightly acidic methanol solution of crown and amine. This complex is mass-selected in the analyzer cell of an FTICR instrument and subjected to activation by soft collisions. This activation is necessary as ESI ionization produces rather cold ions. Propene losses are observed producing the corresponding NH_4^+–crown complex. After re-isolation of this catalytic intermediate, leaking in propylamine leads to a back exchange of NH_3 against propylamine and thus regenerates the initial complex so that a new catalytic cycle can begin.

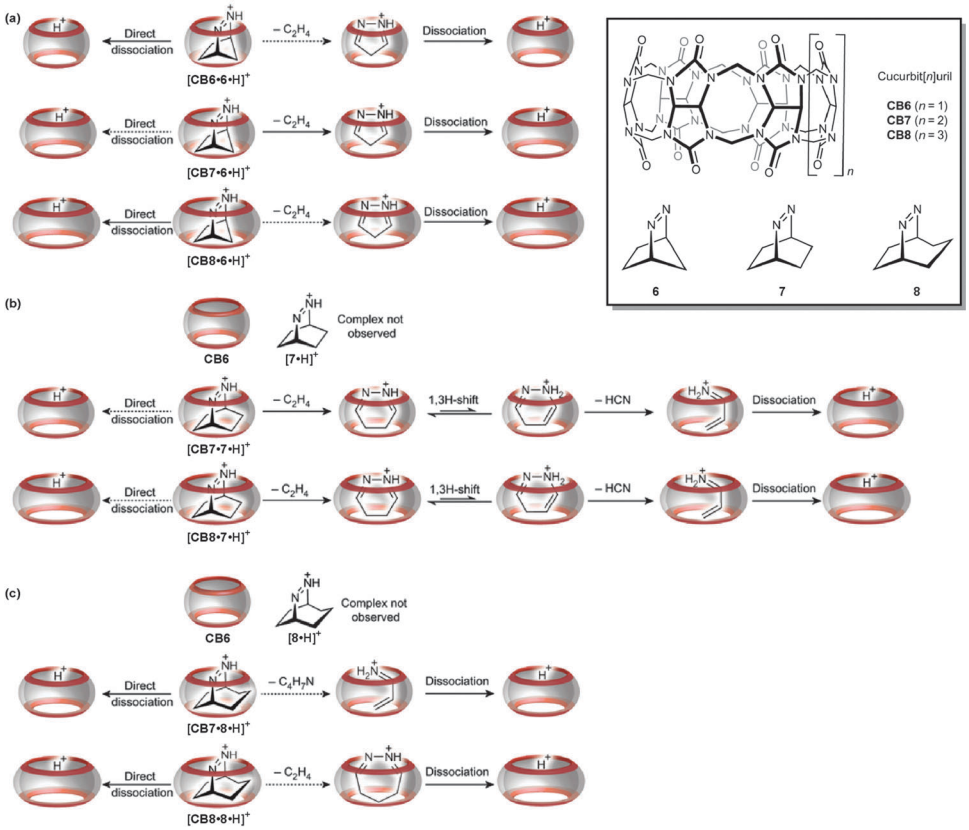

Fig. 4 Depending on the complementarity of guest size with the host's cavity size, guest molecules **6–8** form complexes with cucurbiturils **CB6–CB8**. The dissociation in the gas phase is governed by a competition between complex dissociation and an inner-phase retro-Diels–Alder reaction. The size complementarity decides which process dominates. Reprinted from ref. 22 with permission from the Nature Publishing Group.

Unfortunately, however, each mass-selection step is associated with intensity losses, so that it is not very easy to perform a larger number of cycles in one experiment. This of course limits the scope of the gas-phase approach to some extent.

Fig. 5 shows another experiment: here, all five crown ethers **9–13**, which differ by crown size, were mixed in the same sample solution. Consequently, the propylammonium complexes of all of them are generated simultaneously and can be trapped in the accumulation hexapole of the FTICR instrument. As all ions are reacted under the same conditions, one can at least roughly compare the efficiency with which they undergo propene elimination. Quite obviously, the larger crown ethers **11** and **12** undergo very efficient elimination reactions, while the efficiency decreases for smaller ones. With crown sizes below [24]crown-8, no efficient propene elimination is observed – except for a lariat ether such as **13**, which offers an [18]crown-6 backbone extended by a catalytically active side chain. Similarly, the ammonia–propylamine back-exchange can be compared for all NH_4^+–crown complexes, when the corresponding ammonium complexes are generated and reacted with propylamine in the hexapole in an independent experiment.

From the experiments described here, the catalytic cycle shown in Fig. 5 emerges. Larger crown ethers can easily help activate the β-hydrogen atom and simultaneously offer stabilization and activation to the NH_3 leaving group. Smaller crown ethers are not flexible enough to interact with both parts of the propylamine molecule.

7 Intra- *versus* intermolecular reactivity: metallo-supramolecular complexes

Metallo-supramolecular assemblies which form by error-correcting self-assembly processes in solution usually exhibit highly dynamic intermolecular building block exchange processes. The Stang-type square shown in Fig. 6 equilibrates within minutes, when Pd^{II} is used as the metal ion. With Pt^{II}, the process is slower and the equilibrium is reached within several hours. As any additional reactivity that might occur in solution is superimposed by these often fast exchange reactions, it is not easy – if possible at all – to unambiguously detect it.

In the gas phase, however, these Stang squares are isolated, and therefore, all dynamic exchange processes of building blocks are efficiently suppressed. When one mass-selects the triply or even the quintuply charged square and fragments either one by irradiation with an IR laser in an IRMPD experiment, highly selective fragmentation is observed.[25] Very clearly, the square in both charge states fragments exclusively into a 3 : 3 and a 1 : 1 complex under charge separation, while no fragmentation into two 2 : 2 complexes is observed. This surprising observation can be

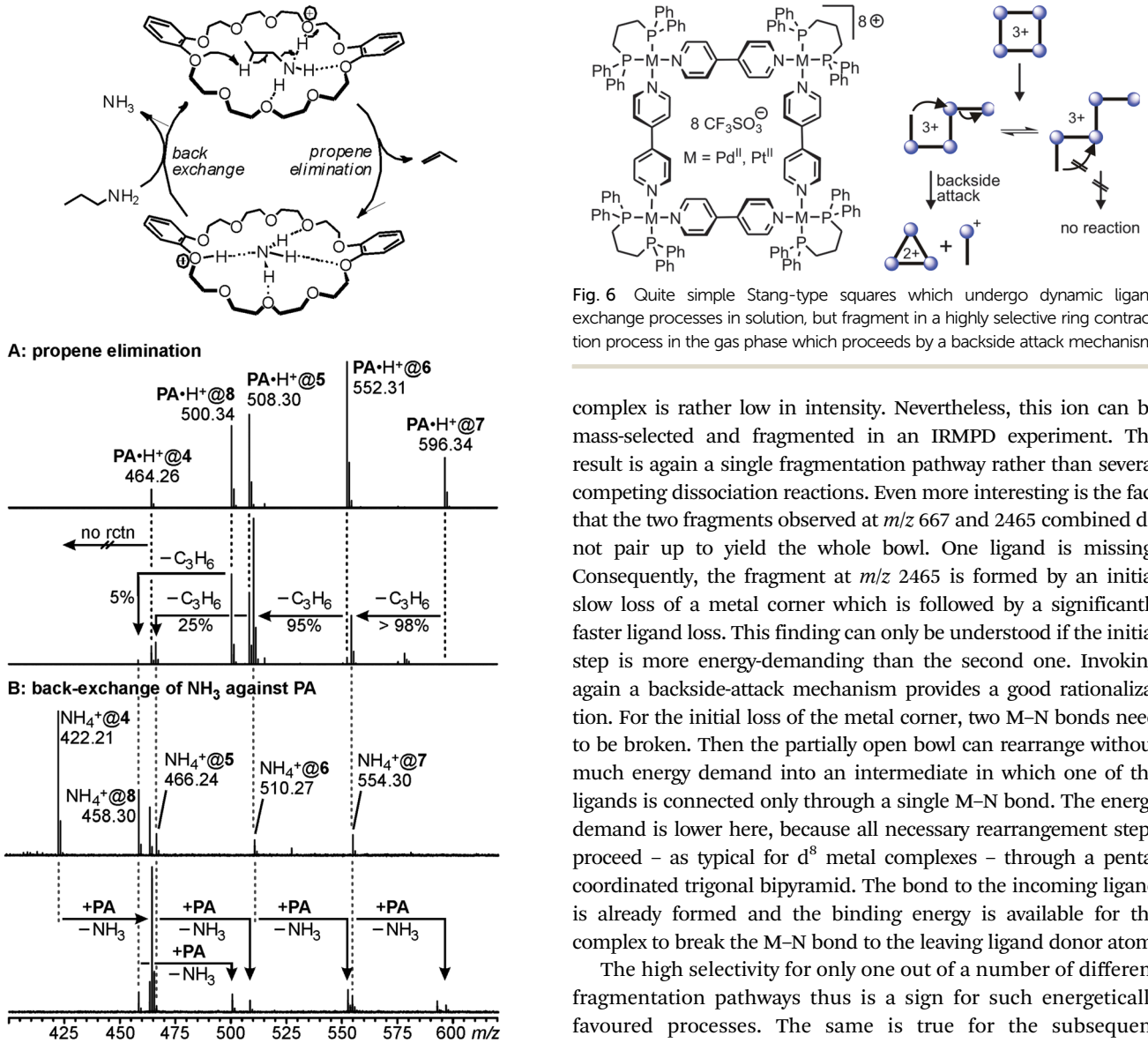

Fig. 5 Larger crown ethers catalyse the elimination of ammonia from alkylamines. Top: catalytic cycle shown exemplarily for dibenzo[30]crown-10 and propylamine. Bottom: mass spectra comparing the efficiency of the two catalytic steps for crown ethers **9–13**.

Fig. 6 Quite simple Stang-type squares which undergo dynamic ligand exchange processes in solution, but fragment in a highly selective ring contraction process in the gas phase which proceeds by a backside attack mechanism.

explained by a mechanism (Fig. 6) which proceeds through an initial ring opening step followed by a backside attack of a free pyridine N atom at the third metal centre. An analogous mechanism is not feasible for the formation of two 2 : 2 complexes because the strain inside a closed 2 : 2 macrocycle would be too high. Therefore, only the observed pathway benefits from bond formation preceding the final M–N bond cleavage.

Analogous processes can also occur in more complicated three-dimensional cage complexes.[26] The building blocks shown in Fig. 7 (top) assemble into a larger bowl-shaped M_6L_4 complex and a smaller M_3L_2 cage in solution. The ESI mass spectrum of the mixture shows prominent signals for the smaller cage in different charge states, while the signal for a triply charged M_6L_4 complex is rather low in intensity. Nevertheless, this ion can be mass-selected and fragmented in an IRMPD experiment. The result is again a single fragmentation pathway rather than several competing dissociation reactions. Even more interesting is the fact that the two fragments observed at *m*/*z* 667 and 2465 combined do not pair up to yield the whole bowl. One ligand is missing. Consequently, the fragment at *m*/*z* 2465 is formed by an initial slow loss of a metal corner which is followed by a significantly faster ligand loss. This finding can only be understood if the initial step is more energy-demanding than the second one. Invoking again a backside-attack mechanism provides a good rationalization. For the initial loss of the metal corner, two M–N bonds need to be broken. Then the partially open bowl can rearrange without much energy demand into an intermediate in which one of the ligands is connected only through a single M–N bond. The energy demand is lower here, because all necessary rearrangement steps proceed – as typical for d^8 metal complexes – through a penta-coordinated trigonal bipyramid. The bond to the incoming ligand is already formed and the binding energy is available for the complex to break the M–N bond to the leaving ligand donor atom.

The high selectivity for only one out of a number of different fragmentation pathways thus is a sign for such energetically favoured processes. The same is true for the subsequent fragmentation of the fragment at *m*/*z* 2465 into the smaller cage and we can again invoke a backside-attack mechanism for the formation of the M_3L_2 complex in the gas phase.

These contraction reactions imply (i) that the formation of a closed triangle in the Stang square case or a small closed cage in the case of the M_6L_3 bowl is energetically feasible and therefore (ii) that the M–N bond must be stronger than the strain that is incorporated in the fragmentation products. These studies show that one should also have an eye for those signals that are expected (here the 2 : 2 complexes) but absent in the MS/MS spectra. Furthermore, they illustrate how reactivity data can help to gain insight into structure and – at least qualitative – energetics.

8 Electron-capture dissociation: one-electron reductions in the gas phase

It is necessary to point out that different activation methods – *i.e.* CID, IRMPD or ECD – may well result in differences in the

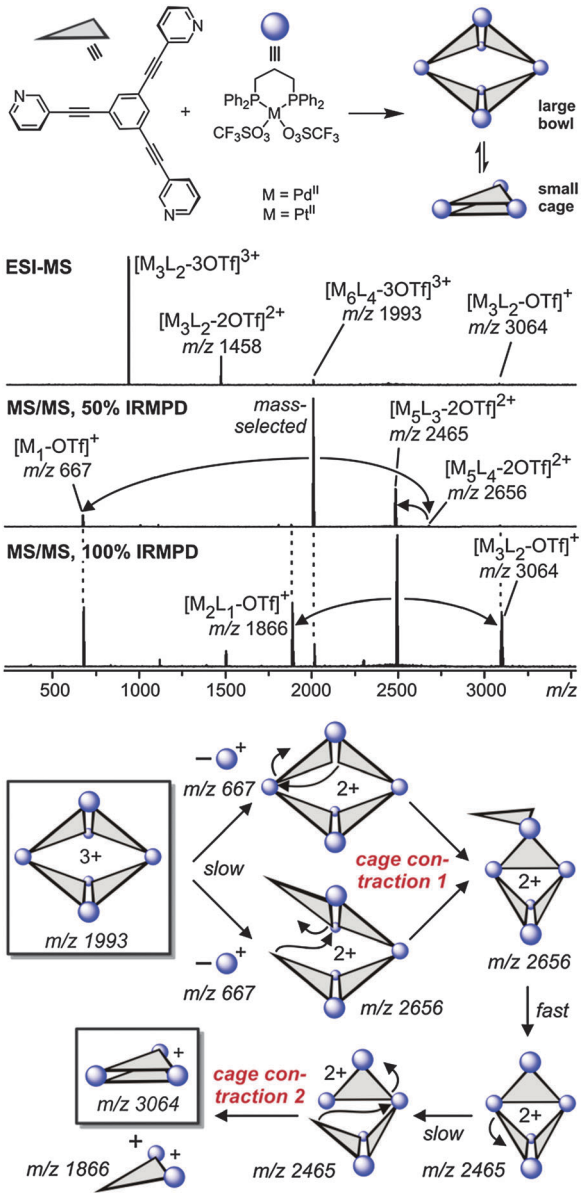

Fig. 7 A double cage contraction in the gas phase leads to surprisingly selective fragmentation pathways. Top: the building blocks form a large M_6L_4 bowl and a smaller M_3L_2 cage in solution as evidenced by NMR experiments. Centre: ESI mass spectrum showing the coexistence of both assemblies in solution and IRMPD experiments performed with the mass-selected $[M_6L_4\text{-}3OTf]^{3+}$ ion (OTf = triflate). Bottom: fragmentation mechanism with two cage-contraction steps.

fragmentation behaviour. Usually, CID and IRMPD give rise to at least qualitatively similar results, although relative intensities of the fragments formed can differ because of differences of the internal energy distributions of the parent ions. Electron capture dissociation, however, is very different in that slow electrons are captured by the multiply positive parent ion. This leads not only to an increase of the parent's internal energy, but also to a one-electron reduction concomitant with the formation of an open-shell cation that exhibits significantly altered reactivity.

Such one-electron reduction reactions in the gas phase have been performed with the triply charged Stang-type square shown in Fig. 6 (M = Pt).[27] In the ECD spectra, the IRMPD-typical fragmentation into a singly charged 1 : 1 and a doubly charged 3 : 3 complex still appears, but only as a minor fragmentation product. The major process instead corresponds to one-electron uptake followed by the loss of two neutral ligands. Consequently, the gas-phase reactivity has more or less completely changed. In order to answer the question whether the electron is located on one of the metal ions or one of the bipyridine ligands,[28] a control experiment with a $(dppp)Pt(NCCH_3)_2^{2+}$ complex was performed. If the electron reduces one of the metal ions incorporated in the square, one would expect to observe one-electron reduction of this complex, too. This is however not the case so that one can conclude the electron to be located on one of the bipyridine ligands, which thus is not a mere spectator, but actively involved in the ECD process.

Another example[29] for an ECD experiment with a metallosupramolecular complex is shown in Fig. 8. Here, a triple-stranded helicate built from three ligands **L1** and two Fe^{II} ions is examined. Electrospray ionization strips off all counterions and the quadruply charged $[Fe_2\mathbf{L1}_3]^{4+}$ ion is subsequently mass-selected as the parent. After 30 ms reaction time, two new signals appear in the mass spectrum: one corresponds to the one-electron reduction product $[Fe_2\mathbf{L1}_3]^{3\bullet+}$, and the second one to the $[Fe_2\mathbf{L1}_2]^{2+}$ ion which has undergone two reduction steps and one ligand loss reaction. Longer reaction times induce consecutive reactions that also involve fragmentations within the ligand. A detailed comparison with double-stranded helicates

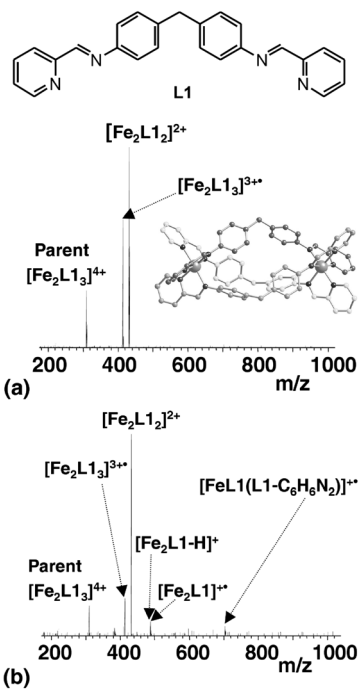

Fig. 8 Top: chemical structure of ligand **L1**. Bottom: ECD spectra of the triply charged triple-stranded Fe^{II} helicate $[Fe_2\mathbf{L1}_3]^{4+}$ after (a) 30 and (b) 70 ms of irradiation with slow electrons. The inset shows the structure of the helicate. Reproduced from ref. 29 with kind permission from Elsevier.

generated with Cu^{I} and Ag^{I} as the metal centres reveals the electron uptake to occur at the metal centre in this case. Quite obviously, a single electron is not sufficient to induce fragmentation, but rather generates a mixed-valence Fe^{II}/Fe^{I} triple stranded helicate. Only the second reduction of the Fe^{I}/Fe^{I} complex is then followed by a ligand loss to yield the double stranded helicate in close analogy to the Cu^{I} and Ag^{I} cases.

9 H/D-exchange reactions in the gas phase: a 1D model for a Grotthus proton transport

As already demonstrated in the section on organocatalysis, bimolecular reactions in the gas phase are possible, for example in ion trap or FTICR instruments, in which ions can be stored over time. A particular bimolecular reaction is the exchange of labile hydrogen atoms against deuterium as this does not change the chemical properties of the ion under study, but its mass. Typically, an H/D-exchange (HDX) reaction proceeds through (i) the formation of an encounter complex of the ion of interest with the deuterated exchange reagent, (ii) proton transfer to the exchange reagent, (iii) an isotope scrambling step, (iv) back transfer of the deuteron, and (v) dissociation of the product complex. This sequence of steps implies that the efficiency with which the HDX occurs depends on the proton affinity difference between the neutral analyte and the exchange reagent. Therefore, the choice of reagent is often very important.[30] There are exceptions, when a second functional group can help mediate the exchange in what was coined a "relay mechanism".[31] Here, the energy-demanding proton transfer can be circumvented by concerted mechanisms.

HDX reactions have been applied to supramolecular complexes in the gas phase only rarely in the past.[32] One example which illustrates the importance of concerted mechanisms is shown in Fig. 9. The bowl-shaped resorcinarene **reso** forms four intramolecular hydrogen bonds that stabilize the bowl conformation. In addition, two of these bowls can dimerize to give rise to a capsule, which is capable of encapsulating small guest cations such as Cs^{+} inside its cavity. Already a while ago, the striking observation was made[33] that the monomeric alkali metal ion complexes undergo only a very slow HDX reaction, while the dimeric capsule is significantly faster. This is surprising, because the monomer bears at least four freely accessible OH hydrogen atoms, while all OH groups are involved in hydrogen bonding in the dimer.

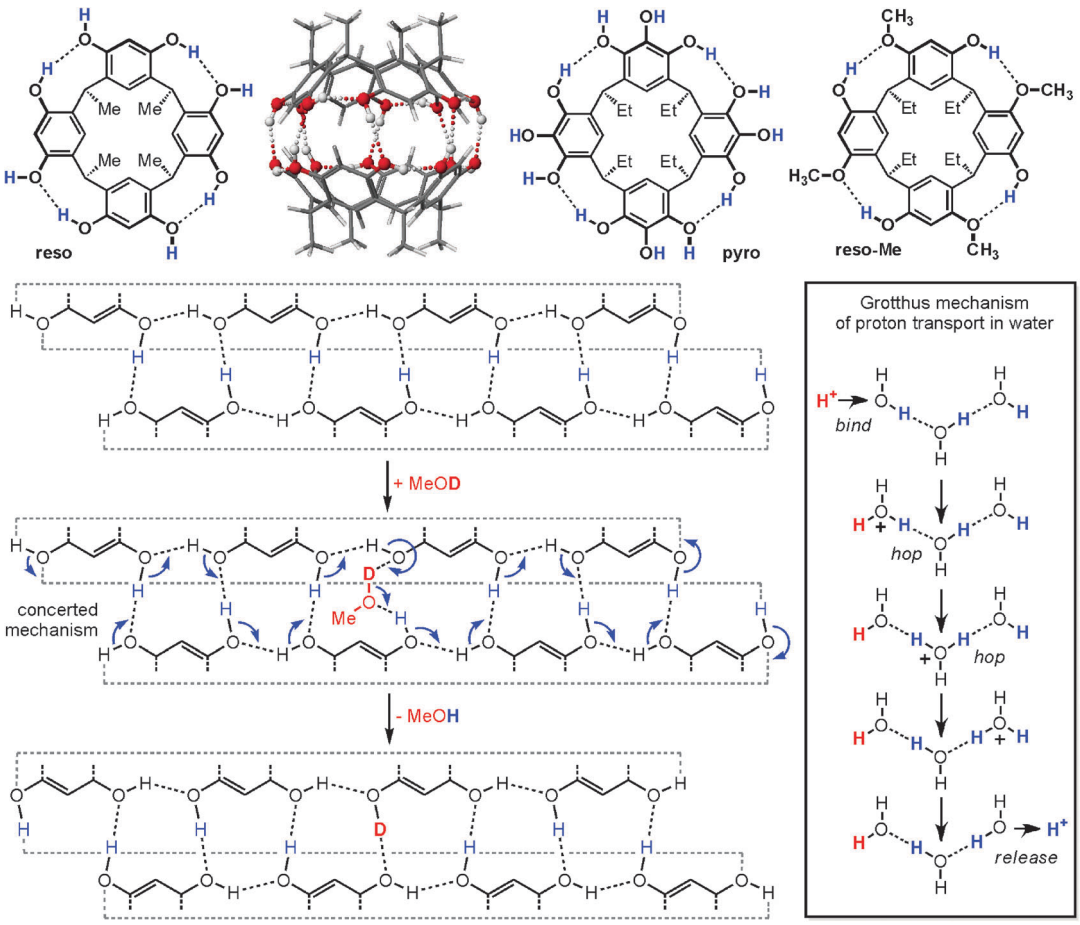

Fig. 9 Top: resorcinarene **reso**, pyrogallarene **pyro** and methylated control compound **reso-Me**. The resorcinarene forms dimeric capsules with, for example, Cs^{+} ions. Bottom left: mercator projection of the hydrogen bonding seam of the dimeric capsule and concerted mechanism for H/D-exchange reactions. Bottom right: analogy to the Grotthus mechanism for proton transport in water.

When one considers the mechanistic details, this behaviour becomes clear:[34] the [**reso**·Cs]$^+$ complex cannot easily undergo a concerted HDX. Consequently, the sequence of steps as described above must proceed through proton transfer intermediates. As the proton affinity difference between a phenolate and methanol-OD as the exchange reagent is extreme, no such reaction can occur. Any concerted mechanism would involve significantly bent H-bonds that are energetically unfavourable.

The fully closed dimer instead can easily undergo the concerted mechanism indicated in Fig. 9 (bottom, left). Insertion of a methanol-OD molecule anywhere in the continuous seam of hydrogen bonds leads to a situation in which only electron pairs need to be shifted. No charge separation step is required. This reaction resembles very much a one-dimensional variant of the Grotthus mechanism for proton transport in water. While it is still under debate whether proton transport in water is concerted or stepwise, the positions of the OH groups in the dimeric resorcinarene capsule are fixed by the scaffold of the two monomers. Thus, the exchange occurs in a concerted way here. A step-wise mechanism would necessarily involve energetically extremely unfavourable charge separation. This is also confirmed by control experiments with **reso-Me** dimers, which do not have a continuous seam of hydrogen bonds and thus do not exhibit any fast HDX reaction. Similarly, cations that are too large to fit inside the capsule such as tetraethyl ammonium break the seam of H-bonds and render the exchange slow. Further experiments with **pyro** dimers reflect the details of the hydrogen bonding patterns and therefore also fit into the mechanistic picture. HDX experiments thus not only provide insight into mechanistic details, but also yield structural information, whether the capsules are fully closed or partially open.

10 Intracomplex dynamics: crown ethers on the spacewalk

The last example for supramolecular gas-phase reactivity to be discussed here tries to answer the question whether gas-phase experiments are able to unravel details about the intramolecular dynamics in supramolecular complexes. More specifically, the question is whether [18]crown-6 can migrate along an oligolysine peptide directly from side chain to side chain (Fig. 10, inset). It is very difficult – if not impossible – to answer this question in a solution study, because one would need to differentiate between the direct migration along the peptide chain and a dissociation–reassociation mechanism. In the gas phase, no such dissociation–reassociation is possible as crown ethers that dissociate will be pumped away in the high vacuum.

Another difficulty must be met in the gas phase, however. Intramolecular processes do not change the mass or the charge

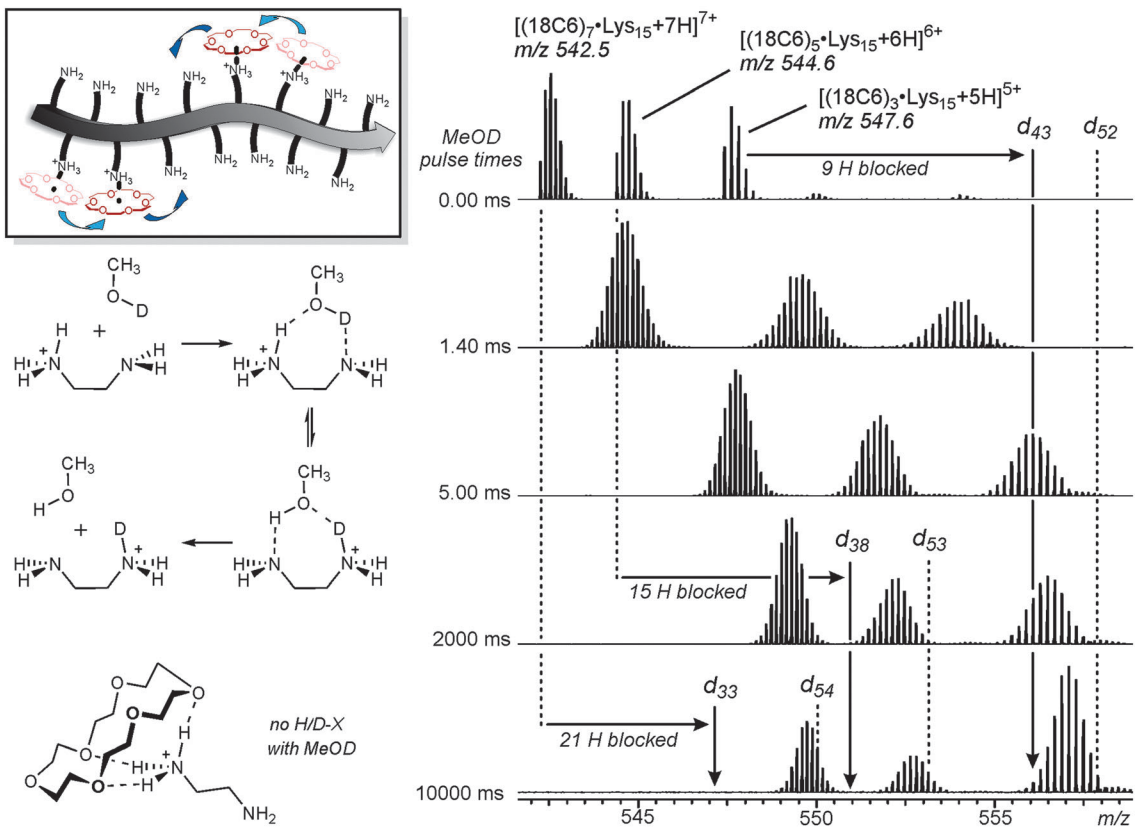

Fig. 10 Top left: the question to be answered: can [18]crown-6 move along an oligolysine peptide by directly hopping from one side chain to another one? Bottom left: the crown ether operates as a non-covalent protective group preventing the HDX reaction on protonated ethylene diamine. Right: HDX reaction on crown–Lys_{15} complexes in different charge states and different stoichiometries.

state of the ion under study. Consequently, they are not visible as the m/z remains constant irrespective of any dynamic rearrangement within an ion.

In the particular case discussed here, the HDX reaction provides a means to detect the movement. It is known[35] that protonated ethylene diamine undergoes a very quick exchange of all five NH hydrogen atoms when reacted with either methanol-OD or ND_3. This reaction is so fast, because it involves the relay mechanism depicted in Fig. 10 (bottom left). In marked contrast, the [18]crown-6 complex of the same ion hardly undergoes any H/D-exchange. Consequently, the crown ether serves as a non-covalent protective group.

The conceptual idea to study the intracomplex dynamics in the crown–peptide complexes is based on this protective group behaviour:[36] if the crown ethers are stationary and cannot leave their positions, the corresponding ammonium protons remain protected and only those groups that are not complexed to a crown ether will undergo the HDX. If the crown is mobile, all protons should be exchangeable. Fig. 10 (right) provides the result. Irrespective of the stoichiometry or the charge state of the complexes, all NH hydrogen atoms can clearly be exchanged and we can thus conclude the crown ether to be able to migrate from side chain to side chain.

Studies with model compounds also resulted in more detailed mechanistic information and revealed the crown ether to move together with a proton from an ammonium site to an amine site in the peptide chain. Furthermore, a comparison of acid- and amide-terminated peptide chains resulted in the conclusion that the acid-terminated crown–peptide complexes are zwitterionic in nature. The HDX behaviour thus even uncovered structural details.

A similar dynamic behaviour was observed in complexes of POPAM dendrimers and crown ethers[37] as well as in complexes of POPAM dendrimers with crown-ether substituted dendrimers.[38]

11 Conclusions

It is the nature of mass spectrometry that structural insight is usually rather indirect compared to other analytical methods. Also, determining solid thermodynamic and kinetic data in the gas phase is not trivial, although a number of methods have been developed and applied also to supramolecules. Certainly, researchers involved in the more applied side of supramolecular chemistry might consider mass spectrometry and gas-phase chemistry of non-covalent complexes to be somewhat far-fetched and of little use to the practitioner, because the conditions under which isolated molecules react in the absence of any environment are certainly drastically different from those encountered in real-world applications.

Nevertheless, when applied together with other techniques, these differences are the reason why mass spectrometry often offers complementary data and thus expands the understanding of the supramolecules' behaviour. It lends support to the conclusions drawn from solution studies because the differences between the data obtained in both states of matter are informative. Gas-phase studies answer new questions on reactivity that occurs beyond the dynamic exchange of building blocks in solution. It opens new views into the reactions that can only compete when the dissociation limit of the complex is elevated due to the significantly stronger non-covalent interactions in the gas phase. It may provide a more detailed picture, because the absence of the environment reduces the complexity of the chemical system under study. Often enough this is the key to high-level theory that complements the gas-phase experiment. As discussed in the organocatalysis section, it may also be an advantage to examine each step in multistep reactions – as encountered in catalytic cycles – separately.

Nevertheless, there are also limitations to be considered. Unspecific binding and the fragmentation of very weak complexes during ionization are only two of the more technical limitations. The most important question when considering the relevance of the gas phase for solution is, how the environment interferes with the intrinsic properties of the complexes under study. To arrive at a clear picture here is not always straightforward, but can certainly be rewarding.

Acknowledgements

We thank Prof. Werner Nau, Jacobs University Bremen, for providing a high-quality version of Fig. 4.

Notes and references

1 C. A. Schalley, *Mass Spectrom. Rev.*, 2001, **20**, 253–309; B. Baytekin, H. T. Baytekin and C. A. Schalley, *Org. Biomol. Chem.*, 2006, **4**, 2825–2841; C. A. Schalley and A. Springer, *Mass Spectrometry and Gas-Phase Chemistry of Non-Covalent Complexes*, Wiley, Hoboken, 2009.

2 M. Hutin, C. A. Schalley, G. Bernardinelli and J. R. Nitschke, *Chem.–Eur. J.*, 2006, **12**, 4069–4076; S. P. Black, A. R. Stefankiewicz, M. M. J. Smulders, D. Sattler, C. A. Schalley, J. R. Nitschke and J. K. M. Sanders, *Angew. Chem., Int. Ed.*, 2013, **52**, 5749–5752.

3 N. K. Beyeh, M. Kogej, A. Åhman, K. Rissanen and C. A. Schalley, *Angew. Chem., Int. Ed.*, 2006, **45**, 5214–5218.

4 S. C. Nanita and R. G. Cooks, *Angew. Chem., Int. Ed.*, 2006, **45**, 554–569; C. A. Schalley and P. Weis, *Int. J. Mass Spectrom.*, 2002, **221**, 9–19.

5 See, for example: I.-H. Chu, H. Zhang and D. V. Dearden, *J. Am. Chem. Soc.*, 1993, **115**, 5736–5744; P. D. Schnier, J. S. Klassen, E. F. Strittmatter and E. R. Williams, *J. Am. Chem. Soc.*, 1998, **120**, 9605–9613; P. B. Armentrout, *Int. J. Mass Spectrom.*, 1999, **193**, 227–240; E. C. Kempen and J. S. Brodbelt, *Anal. Chem.*, 2000, **72**, 5411–5416; J. D. Anderson, E. S. Paulsen and D. V. Dearden, *Int. J. Mass Spectrom.*, 2003, **227**, 63–76.

6 See, for example: P. F. James, M. A. Perugini and R. A. J. O'Hair, *J. Am. Soc. Mass Spectrom.*, 2006, **17**, 384–394; Y. Xia, X. Liang and S. A. McLuckey, *Anal. Chem.*, 2006, **78**, 1218–1227; W. Danikiewicz, P. Tarnowski, T. Bienkowski and J. Jurczak, *Pol. J. Chem.*, 2004, **78**,

699–709; V. J. Nesatyy and J. Laskin, *Int. J. Mass Spectrom.*, 2002, **221**, 245–262; H.-F. Wu and J. S. Brodbelt, *J. Am. Soc. Mass Spectrom.*, 1993, **4**, 718–722; C. C. Liou and J. S. Brodbelt, *J. Am. Chem. Soc.*, 1992, **114**, 6761–6764.

7 S. Sakamoto, M. Fujita, K. Kim and K. Yamaguchi, *Tetrahedron*, 2000, **56**, 955–964.

8 H. N. Miras, E. F. Wilson and L. Cronin, *Chem. Commun.*, 2009, 1297–1311.

9 I. Prat, J. S. Mathieson, M. Güell, J. M. Luis, L. Cronin and M. Costas, *Nat. Chem.*, 2011, **3**, 788–793.

10 T. Liebig, U. Lüning and J. Grotemeyer, *Eur. J. Mass Spectrom.*, 2006, **12**, 117–120; J. Taubitz, U. Lüning and J. Grotemeyer, *Chem. Commun.*, 2004, 2400–2401.

11 A. G. Marshall, C. L. Hendrickson and G. S. Jackson, *Mass Spectrom. Rev.*, 1998, **17**, 1–35; R. T. McIver Jr. and J. R. McIver, *Fourier Transform Mass Spectrometry - Principles and Applications*, IonSpec, Lake Forest, 2006.

12 T. Karpuschkin, M. M. Kappes and O. Hampe, *Angew. Chem., Int. Ed.*, 2013, **52**, 10374–10377; O. Hampe, T. Karpuschkin, M. Vonderach, P. Weis, Y. Yu, L. Gan, W. Klopper and M. M. Kappes, *Phys. Chem. Chem. Phys.*, 2011, **13**, 9818–9823; O. P. Balaj, C. B. Berg, S. J. Reitmeiuer, V. E. Bondybey and M. K. Beyer, *Int. J. Mass Spectrom.*, 2009, **279**, 5–9.

13 H. D. F. Winkler, E. V. Dzyuba and C. A. Schalley, *New J. Chem.*, 2011, **35**, 529–541.

14 T. Wyttenbach, P. R. Kemper and M. T. Bowers, *Int. J. Mass Spectrom.*, 2001, **212**, 13–23; G. A. Eiceman and Z. Karpas, *Ion Mobility Spectrometry*, CRC press, Boca Raton, 1994.

15 E. R. Brocker, S. E. Anderson, B. H. Northrop, P. J. Stang and M. T. Bowers, *J. Am. Chem. Soc.*, 2010, **132**, 13486–13494; J. Ujma, M. De Cecco, O. Chepelin, H. Levene, C. Moffat, S. J. Pike, P. J. Lusby and P. E. Barran, *Chem. Commun.*, 2012, **48**, 4423–4425; P. J. Robbins, A. J. Surman, J. Thiel, D.-J. Long and L. Cronin, *Chem. Commun.*, 2013, **49**, 1909–1911.

16 S. Myung, M. Fioroni, R. R. Julian, S. L. Koeniger, M. H. Baik and D. E. Clemmer, *J. Am. Chem. Soc.*, 2006, **128**, 10833–10839; R. R. Julian, R. Hodyss, B. Kinnear, M. F. Jarrold and J. L. Beauchamp, *J. Phys. Chem. B*, 2002, **106**, 1219–1228.

17 C. A. Schalley, C. Verhaelen, F.-G. Klärner, U. Hahn and F. Vögtle, *Angew. Chem., Int. Ed.*, 2005, **44**, 477–480.

18 W. Jiang and C. A. Schalley, *J. Mass Spectrom.*, 2010, **45**, 788–798; W. Jiang, H. D. F. Winkler and C. A. Schalley, *J. Am. Chem. Soc.*, 2008, **130**, 13852–13853; W. Jiang and C. A. Schalley, *Proc. Natl. Acad. Sci. U. S. A.*, 2009, **106**, 10425–10429; W. Jiang, P. C. Mohr, A. Schäfer and C. A. Schalley, *J. Am. Chem. Soc.*, 2010, **132**, 2309–2320; W. Jiang, Q. Wang, I. Linder, F. Klautzsch and C. A. Schalley, *Chem.–Eur. J.*, 2011, **17**, 2344–2348.

19 R. R. Julian, J. A. May, B. M. Stoltz and J. L. Beauchamp, *Angew. Chem., Int. Ed.*, 2003, **42**, 1012–1015; M. Schäfer, *Angew. Chem., Int. Ed.*, 2003, **42**, 1896–1899.

20 E. Masson, X. Ling, R. Joseph, L. Kyeremeh-Mensah and X. Lu, *RSC Adv.*, 2012, **2**, 1213–1247.

21 B. C. Pemberton, R. Raghunathan, S. Volla and J. Sivaguru, *Chem.–Eur. J.*, 2012, **18**, 12178–12190.

22 T.-C. Lee, E. Kalenius, A. I. Lazar, K. I. Assaf, N. Kuhnert, C. H. Grün, J. Jänis, O. A. Scherman and W. M. Nau, *Nat. Chem.*, 2013, **5**, 376–382.

23 K. Eller and H. Schwarz, *Chem. Rev.*, 1991, **91**, 1121–1177; D. A. Plattner, *Top. Curr. Chem.*, 2003, **225**, 153–203.

24 H. D. F. Winkler, E. V. Dzyuba, A. Springer, L. Losensky and C. A. Schalley, *Chem. Sci.*, 2012, **3**, 1111–1120.

25 C. A. Schalley, T. Müller, P. Linnartz, M. Witt, M. Schäfer and A. Lützen, *Chem.–Eur. J.*, 2002, **8**, 3538–3551; M. Engeser, A. Rang, M. Ferrer, A. Gutiérrez, H. T. Baytekin and C. A. Schalley, *Int. J. Mass Spectrom.*, 2006, **255–256**, 185–194.

26 B. Brusilowskij, S. Neubacher and C. A. Schalley, *Chem. Commun.*, 2009, 785–787.

27 R. Hovorka, M. Engeser and A. Lützen, *Int. J. Mass Spectrom.*, 2013, **354**, 152–158.

28 K. A. Malgorzata and H. J. Cooper, *Chem. Commun.*, 2011, **47**, 418–420; T. Song, C. N. W. Lam, D. C. M. Ng, G. Orlova, J. Laskin, D.-C. Fang and I. K. Chua, *J. Am. Soc. Mass Spectrom.*, 2009, **20**, 972–984.

29 M. A. Kaczorowska, A. C. G. Hotze, M. J. Hannon and H. J. Cooper, *J. Am. Soc. Mass Spectrom.*, 2010, **21**, 300–309. Also, see: M. A. Kaczorowska and H. Cooper, *J. Am. Soc. Mass Spectrom.*, 2009, **20**, 674–681.

30 E. Gard, D. Willard, J. Bregar, M. K. Green and C. B. Lebrilla, *Org. Mass Spectrom.*, 1993, **28**, 1632–1639; B. E. Winger, K. J. Light-Wahl, A. L. Rockwood and R. D. Smith, *J. Am. Chem. Soc.*, 1992, **114**, 5897–5898.

31 T. Wyttenbach and M. T. Bowers, *J. Am. Soc. Mass Spectrom.*, 2009, **10**, 9–14; O. Geller and C. Lifshitz, *J. Phys. Chem.*, 2003, **107**, 5654–5659; H. A. Cox, R. R. Julian, S. W. Lee and J. L. Beauchamp, *J. Am. Chem. Soc.*, 2004, **126**, 6485–6490.

32 For a few examples, see: E. Kalenius, D. Moiani, E. Dalcanale and P. Vainiotalo, *Chem. Commun.*, 2007, 3865–3867; Z. Takáts, S. C. Nanita, G. Schlosser, K. Vekey and R. G. Cooks, *Anal. Chem.*, 2003, **75**, 6147–6154.

33 M. Mäkinen, P. Vainiotalo and K. Rissanen, *J. Am. Soc. Mass Spectrom.*, 2002, **13**, 581–583.

34 H. D. F. Winkler, E. V. Dzyuba, J. A. W. Sklorz, N. K. Beyeh, K. Rissanen and C. A. Schalley, *Chem. Sci.*, 2011, **2**, 615–624.

35 S.-W. Lee, H.-N. Lee, H. S. Kim and J. L. Beauchamp, *J. Am. Chem. Soc.*, 1998, **120**, 5800–5805.

36 D. P. Weimann, H. D. F. Winkler, J. A. Falenski, B. Koksch and C. A. Schalley, *Nat. Chem.*, 2009, **1**, 573–577.

37 H. D. F. Winkler, D. P. Weimann, A. Springer and C. A. Schalley, *Angew. Chem., Int. Ed.*, 2009, **48**, 7246–7250.

38 Z. Qi, C. Schlaich and C. A. Schalley, *Chem.–Eur. J.*, 2013, **19**, 14867–14875.

